

**Figure 1.**  $\text{Co}_2\text{NO}^+ + \text{O}_2 \rightarrow \text{Co}_2\text{O}_2^+ + \text{NO}$  studied as a function of time with and without irradiation. The smooth curves represent optimized biexponential fits to the data.

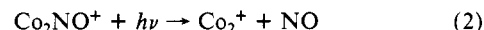
duced dissociation (CID)<sup>7</sup> to remove the CO ligands.  $\text{Co}_2\text{NO}^+$  was generated in the FTMS-2000 by electron impact ionization of  $\text{Co}(\text{CO})_3\text{NO}$  followed by clustering reactions of the ions with the parent neutral and subsequent CID. Swept double resonance techniques<sup>8</sup> were used to isolate the ion of interest.  $\text{Co}(\text{CO})_3\text{NO}$  was introduced through General Valve Series 9 pulsed valves.<sup>9</sup> Utilizing Varian leak valves,  $\text{O}_2$  was maintained at a relatively low pressure,  $\sim 10^{-7}$  Torr, while argon was maintained at a relatively high pressure,  $\sim 10^{-5}$  Torr, to provide collisional cooling for ion thermalization<sup>10</sup> and to act as a collision gas for CID. The FTMS-1000 has been modified as previously described<sup>11</sup> for photochemical studies using a 2500 W Hg-Xe arc lamp. A Spectra Physics Model 2030 high power  $\text{Ar}^+$  laser and a Quanta Ray Nd:YAG laser were used to perform photochemical experiments on the FTMS-2000.

The time between collisions in the low-pressure environment of an FT-ICR-MS dictates that internal conversion, photodissociation, or collisional and radiative relaxation of photoexcited ions can compete favorably with reactive collisions, significantly reducing the possibility of observing a photoinduced ion-molecule reaction pathway under these conditions. However, two examples of such photoenhanced reactivity have been reported.<sup>5,12</sup> These reactions were driven by the vibrational excitation of the reactant ion arising from photon absorption and internal conversion. Recently, we proposed that an alternative photoinduced reaction mechanism could involve changes in reactivity due to photoisomerization.

In this study we observed the reaction of  $\text{Co}_2\text{NO}^+$  with  $\text{O}_2$  as a function of time with and without irradiation. Figure 1 displays the relative abundances of  $\text{Co}_2\text{NO}^+$  and  $\text{Co}_2\text{O}_2^+$  under these conditions. Jacobson has demonstrated that the populations of the reactant and product ions approach an asymptotic limit with increasing time when no irradiation is present. However, when irradiated with 1064-nm ( $\sim 27$  kcal/mol) photons from a pulsed Nd:YAG laser operated at 10 Hz, the nonreactive isomer is observed to become reactive, presumably because the photoexcited species can access both the reactive and the nonreactive isomers. During the original study, Jacobson determined that  $\sim 55\%$  of the thermalized  $\text{Co}_2\text{NO}^+$  population exists in the reactive form. In this study, the  $\text{Co}_2\text{O}_2^+$  produced during the  $\text{Co}_2\text{NO}^+$  synthesis

and isolation period was not ejected from the cell in an effort to prevent inadvertent excitation of  $\text{Co}_2\text{NO}^+$ . When the data in Figure 1 are corrected for this initial  $\text{Co}_2\text{O}_2^+$  population, the reactive isomer accounts for  $\sim 65\%$  of the  $\text{Co}_2\text{NO}^+$  present immediately following isolation. Relative abundances in Figure 1 do not sum to 100% due to a small photodissociation contribution not displayed.

Experiments using arc lamp irradiation at  $\sim 35$  kcal/mol resulted in competition between the photoinduced reactivity characterized in Figure 1 and photodissociation, reaction 2. The



514.5-nm output from the  $\text{Ar}^+$  laser produced photodissociation products exclusively. In a continuing series of studies, we are using variable energy light sources in conjunction with this photoinduced reaction to characterize the height of the  $\text{Co}_2\text{NO}^+$  reactive/nonreactive isomerization barrier. In addition, photodissociation threshold studies are underway to determine  $D(\text{Co}_2^+-\text{NO})$  for the reactive and nonreactive isomers as well as  $D(\text{Co}_2^+-\text{O}_2)$ .

The photoisomerization mechanism is supported by recent collisional activation studies performed by Jacobson<sup>3d</sup> in which the reactive isomer was permitted to react to completion with  $\text{O}_2$ , and the  $\text{Co}_2\text{O}_2^+$  produced was ejected from the cell to isolate the nonreactive isomer of  $\text{Co}_2\text{NO}^+$ . Collisional activation of the nonreactive isomer imparts sufficient internal energy to this species to permit it to access the reactive form. This collision-induced isomerization is consistent with our photoinduced reaction mechanism.

The chemistry exhibited by this system may prove to have far reaching ramifications in the study of the reactivity and photoactivation of molecules on metal microsurfaces, particularly concerning the question of molecular vs dissociative chemisorption. The search for additional examples of photoinduced ion-molecule reactions in the gas phase continues in our laboratory.

**Acknowledgment** is made to the Division of Chemical Sciences, Office of Basic Energy Sciences, United States Department of Energy (DE-FG02-87ER13776) for supporting transition-metal ion research and to the National Science Foundation (CHE-8612234) for continued support of FT-ICR-MS instrumentation. J.R.G. gratefully acknowledges the National Science Foundation for predoctoral fellowship support and Lance Safford for many helpful discussions.

## Multielectron Redox Reactions between Manganese Porphyrins Mediated by Nitrogen Atom Transfer

L. Keith Woo\* and James G. Goll

Department of Chemistry, Iowa State University  
Ames, Iowa 50011

Received November 2, 1988

From the pioneering work of Taube,<sup>1</sup> electron-transfer reactions can be mechanistically categorized into either inner sphere or outer sphere processes. The most well-studied systems in either case typically involve one-electron changes. Redox processes involving transfers of a multiple number of electrons, especially between two metals, are much less prevalent and consequently less well understood. The most extensive studies on multiple electron changes have involved atom transfer processes.<sup>2</sup> These are typically two electron-transfer reactions mediated by either a bridging halogen<sup>3,4</sup> or a bridging oxo<sup>5</sup> ligand. The consideration

(6) Cody, R. B.; Burnier, R. C.; Reents, W. D., Jr.; Carlin, T. J.; McCrery, D. A.; Lengel, R. K.; Freiser, B. S. *Int. J. Mass Spectrom. Ion Phys.* **1980**, *33*, 37.

(7) Cody, R. B.; Freiser, B. S. *Int. J. Mass Spectrom. Ion Phys.* **1982**, *41*, 199.

(8) Comisarow, M. B.; Parisod, G.; Grassi, V. *Chem. Phys. Lett.* **1978**, *57*, 413.

(9) Carlin, T. J.; Freiser, B. S. *Anal. Chem.* **1983**, *55*, 571.

(10) Kang, H.; Beauchamp, J. L. *J. Phys. Chem.* **1985**, *89*, 3364.

(11) Hettich, R. L.; Jackson, T. C.; Stanko, E. M.; Freiser, B. S. *J. Am. Chem. Soc.* **1986**, *108*, 5086.

(12) Bomse, D. S.; Beauchamp, J. L. *J. Am. Chem. Soc.* **1980**, *102*, 3967.

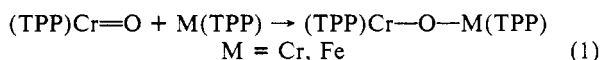
(1) (a) Taube, H.; Myers, H.; Rich, R. L. *J. Am. Chem. Soc.* **1953**, *75*, 4118. (b) Taube, H.; Myers, H. *J. Am. Chem. Soc.* **1954**, *76*, 2103.

(2) Taube, H. In *Mechanistic Aspects of Inorganic Reactions*; ACS Symposium Series 198; Rorabacher, D. B., Endicott, J. F., Eds.; American Chemical Society: Washington, DC, 1982; Chapter 7.

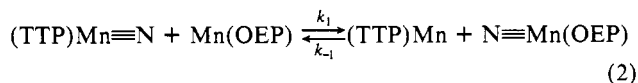
(3) (a) Basolo, F.; Wilks, P. H.; Pearson, R. G.; Wilkins, R. G. *J. Inorg. Nucl. Chem.* **1958**, *6*, 161. (b) Johnson, R. C.; Basolo, R. *J. Inorg. Nucl. Chem.* **1960**, *13*, 36. (c) Basolo, F.; Morris, M. L.; Pearson, R. G. *Discuss. Faraday Soc.* **1960**, *29*, 80. (d) Cox, L. T.; Collins, S. B.; Martin, D. S., Jr. *J. Inorg. Nucl. Chem.* **1961**, *17*, 383.

of a nitrido ligand as a bridging species in redox reactions has received little attention.<sup>6</sup> In this regard, we initiated studies on the bridging capabilities of the nitrido complexes of metalloporphyrins. We report herein the first example of a reversible net three electron redox process mediated by nitrogen atom transfer.

Given the stability of  $\mu$ -nitrido iron porphyrin dimers,<sup>7,9c</sup> it seemed likely that analogous manganese complexes may also exist. When  $(\text{TTP})\text{Mn}\equiv\text{N}$ <sup>8,9</sup> is treated with  $\text{Mn}(\text{TTP})$ <sup>10</sup> in toluene under anaerobic conditions, the UV-vis spectrum of the mixture showed only Soret bands at 422 nm (nitrido complex) and 435 nm ( $\text{Mn}^{\text{II}}$  complex), indicating that the predominant species in solution are monomeric. Formation of stable  $\mu$ -nitrido complexes in any appreciable amounts should have resulted in the appearance of a new Soret band. This behavior is in contrast to the oxo chemistry of metalloporphyrins. For example, treating  $(\text{TPP})\text{Cr}=\text{O}$  with  $\text{M}(\text{TPP})$ ,  $\text{M} = \text{Cr}, \text{Fe}$ , results in the formation of  $\mu$ -oxo dinuclear complexes as shown in eq 1.<sup>11</sup>



Clearly, nitrido bridged manganese porphyrin complexes are unstable relative to the monomers. Nevertheless, formation of such a species in solution, albeit in undetectable concentrations, could lead to nitrogen atom transfer. In order to examine this possibility, a labeling experiment was performed in which a different porphyrin was used on one of the complexes. Thus, when toluene solutions of  $(\text{TTP})\text{Mn}\equiv\text{N}$  and  $\text{Mn}(\text{OEP})$  were added together under anaerobic conditions, the UV-vis spectrum of the mixture showed new Soret bands at 404 and 435 nm. This is consistent with the formation of  $(\text{OEP})\text{Mn}\equiv\text{N}$  (404 nm) and  $\text{Mn}(\text{TTP})$  (435 nm). Independent verification of this was obtained by an NMR study. Under vacuo, toluene-*d*<sub>8</sub> was condensed into an NMR tube containing a 1:1 mixture of solid  $\text{N}\equiv\text{Mn}(\text{TTP})$  and  $\text{Mn}(\text{OEP})$  at  $-78^\circ\text{C}$ . After flame sealing the tube and warming to ambient temperature, a 300 MHz  $^1\text{H}$  NMR spectrum was taken. The manganese(V) nitride complexes are diamagnetic and easily detected by NMR. Thus, the appearance of new peaks at  $\delta$  10.29 (s, 4 H, meso H), 3.97 (m, 16 H,  $\text{CH}_2$ ), and 1.85 (t, 24 H,  $\text{CH}_3$ ) indicated the formation of a new nitride complex,  $\text{N}\equiv\text{Mn}(\text{OEP})$ . The complementary experiments, in which solutions of  $\text{N}\equiv\text{Mn}(\text{OEP})$  and  $\text{Mn}(\text{TTP})$  are combined, result in the formation of  $\text{N}\equiv\text{Mn}(\text{TTP})$  and indicate that this process is reversible. The overall reaction is illustrated in eq 2. This



represents the first example of nitrogen atom transfer—formally a three-electron redox process. The equilibrium constant for this reaction as written in eq 2 was determined by  $^1\text{H}$  NMR and UV-vis spectroscopy and is  $1.7 \pm 0.7$  at  $20.0 \pm 0.1^\circ\text{C}$ .

Rates for nitrogen atom exchange were measured spectrophotometrically by following absorbance changes at 403 nm using a Cary 17 spectrophotometer equipped with a thermostatted cell holder which was maintained at  $20.0 \pm 0.1^\circ\text{C}$ . Treatment of

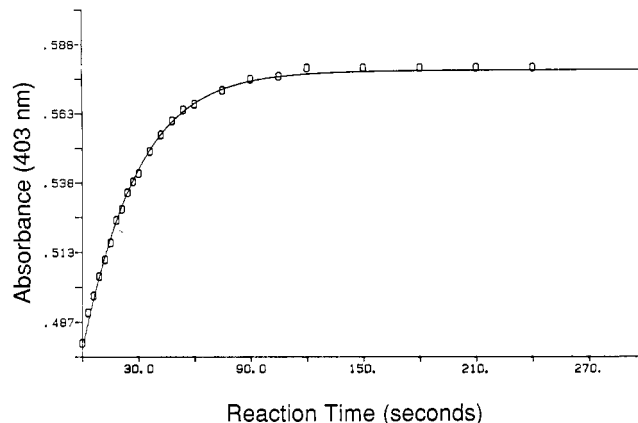
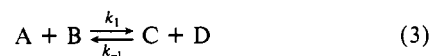


**Figure 1.** Representative plot of  $A_{403}$  versus time used for the determination of  $k_1$ .  $[\text{N}\equiv\text{Mn}(\text{TTP})]_0 = 3.39 \times 10^{-6} \text{ M}$  and  $[\text{Mn}(\text{OEP})]_0 = 3.40 \times 10^{-6} \text{ M}$ . The open circles are experimentally determined data points, and the solid curve was calculated using eq 4.

the kinetic data was accomplished with an integrated rate law for reversible reactions derived by King.<sup>12</sup> This analysis utilizes a variable,  $\Delta$ , which represents the displacement of a reactant's concentration at a given time,  $t$ , from its equilibrium value,  $t = \infty$ . Hence, reaction 3



is characterized by the integrated rate law

$$\ln \left[ \frac{\Delta}{\alpha + \Delta(1 - 1/K)} \right] = -k_1 \alpha t + \text{const} \quad (4)$$

where  $\alpha = [\text{A}]_\infty + [\text{B}]_\infty + \{([\text{C}]_\infty + [\text{D}]_\infty)/K\}$  and  $\Delta = [\text{A}]_t - [\text{A}]_\infty = [\text{B}]_t - [\text{B}]_\infty = [\text{C}]_t - [\text{C}]_\infty = [\text{D}]_t - [\text{D}]_\infty$ .

A series of kinetics runs were performed in which the initial concentrations of the starting reagents were varied from  $1.13 \times 10^{-6}$  to  $1.04 \times 10^{-5} \text{ M}$ . In addition, the initial starting concentration ratios of the nitrido complex to the  $\text{Mn}(\text{II})$  complex were varied from approximately 1:1 to 1:5. A representative plot of absorbance versus time used for the determination of rates is shown in Figure 1. When reactions were run with  $(\text{TTP})\text{Mn}\equiv\text{N}$  and  $\text{Mn}(\text{OEP})$  as the starting reactants, similar rate constants were obtained regardless of the initial concentrations or ratios used. This strongly suggests that the nitrogen atom transfer process in eq 2 obeys the integrated rate law eq 4 and is first order in each reactant. This kinetic behavior is analogous to that found for the nitrogen atom transfer reaction between  $(\text{OEP})\text{Mn}\equiv\text{N}$  and  $\text{Cl}-\text{Cr}(\text{TPP})$  reported by Bottomley.<sup>6</sup>

The second-order rate constant for transfer of the nitrogen atom from  $(\text{TTP})\text{Mn}\equiv\text{N}$  to  $\text{Mn}(\text{OEP})$  is  $k_1 = 4.2 (\pm 1.6) \times 10^3 \text{ M}^{-1} \text{ s}^{-1}$ . A similar set of experiments were carried out for eq 2 in the reverse direction, establishing  $k_{-1}$  as  $2.8 (\pm 0.7) \times 10^3 \text{ M}^{-1} \text{ s}^{-1}$ . This is in good agreement with the value expected from  $k_1/K_{\text{eq}}$  ( $2.3 \times 10^3 \text{ M}^{-1} \text{ s}^{-1}$ ). These nitrogen atom transfer rates are remarkably fast and are surprising in light of the fact that the high spin  $d^5$  manganese reductant must undergo a spin quantum number change on becoming the low spin  $d^2$  nitridomanganese complex. In comparison, a spin change argument has been used to rationalize the extremely slow rates for the oxidation of high spin  $\text{Co}^{2+}$  to low spin  $\text{Co}^{3+}$ .<sup>13</sup>

We are currently undertaking analogous studies with chromium porphyrins and attempting to determine the scope and generality of nitrogen atom transfer. Further work is also in progress to examine the differences between the oxo and nitrido chemistry of metalloporphyrins.

**Acknowledgment.** Financial support for this work was provided by the Research Corporation and a University Research Grant

(4) Smith, T. P.; Iverson, D. J.; Droege, M. W.; Kwan, K. S.; Taube, H. *Inorg. Chem.* **1987**, *26*, 2882.

(5) Holm, R. H. *Chem. Rev.* **1987**, *87*, 1401.

(6) Bottomley, L. A.; Neely, F. L. *J. Am. Chem. Soc.*, in press.

(7) Summerville, D. A.; Cohen, I. A. *J. Am. Chem. Soc.* **1976**, *98*, 1747.

(8) Abbreviations: TTP = 5,10,15,20-tetra-*p*-tolylporphyrinato dianion; TPP = 5,10,15,20-tetraphenylporphyrinato dianion; OEP = 2,3,7,8,12,13,17,18-octaethylporphyrinato dianion.

(9) (a) Hill, C. L.; Hollander, F. J. *J. Am. Chem. Soc.* **1982**, *104*, 7318.

(b) Groves, J. T.; Takahashi, T. *J. Am. Chem. Soc.* **1983**, *105*, 2073. (c) Buchler, J. W.; Dreher, C. Z. *Naturforsch.* **1984**, *39B*, 222. (d) Buchler, J. W.; Dreher, C.; Lay, K. L. *Z. Naturforsch.* **1982**, *37B*, 1155.

(10) Reed, C. A.; Kouba, J. K.; Grimes, C. J.; Cheung, S. K. *Inorg. Chem.* **1978**, *17*, 2666.

(11) (a) Liston, D. J.; Murray, K. S.; West, B. O. *J. Chem. Soc. Chem. Commun.* **1982**, 1109. (b) Liston, D. J.; Kennedy, B. J.; Murray, K. S.; West, B. O. *Inorg. Chem.* **1985**, *24*, 1561. (c) Liston, D. J.; West, B. O. *Inorg. Chem.* **1985**, *24*, 1568.

(12) King, E. L. *Int. J. Chem. Kinet.* **1982**, *14*, 1285.

(13) Stynes, H. C.; Ibers, J. A. *Inorg. Chem.* **1971**, *10*, 2304.

administered by Iowa State University. We thank Professor James H. Espenson for directing us to E. L. King's kinetic treatment and for the loan of a thermostatable cell holder and a constant temperature bath, Dr. Dave Scott for assistance with the NMR experiments, and J. Alan Hays for help with computer software used in data manipulation.

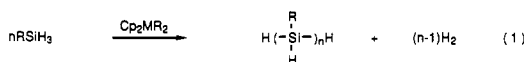
## $\sigma$ -Bond Metathesis Reactions of Si-H and M-Si Bonds. New Routes to d<sup>0</sup> Metal Silyl Complexes

Hee-Gweon Woo and T. Don Tilley\*

Chemistry Department, D-006  
University of California at San Diego  
La Jolla, California 92093-0506

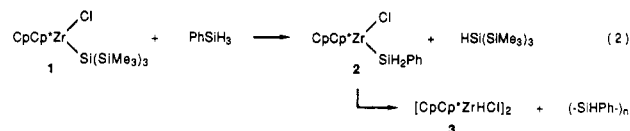
Received December 27, 1988

The recent development of early transition-metal silyl chemistry has resulted in observation of a number of unusual chemical transformations.<sup>1</sup> For example, the catalytic dehydrogenative polymerization of silanes to polysilanes by Ti and Zr metallocene derivatives<sup>2</sup> (eq 1) has generated much interest, since routes to



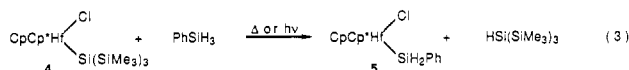
these polymers are presently quite limited.<sup>3</sup> More versatile synthetic methods are expected to promote development of a number of applications for polysilanes, for example as photoreists,<sup>4a,b</sup> photoconductors,<sup>4c</sup> dopable semiconductors,<sup>4d</sup> preceramics,<sup>4e-g</sup> and nonlinear optical materials.<sup>4h</sup> The newly discovered coordination polymerization (eq 1) undoubtedly involves metal-silicon bonded intermediates with Si-H bonds, but the mechanism is still very much in question.<sup>2b-d</sup> Here we report stoichiometric  $\sigma$ -bond metathesis reactions that are possibly related to the initiation process of the polymerization. The reactions described also provide a new, general route to d<sup>0</sup> metal silyl complexes with  $\alpha$  Si-H bonds. Such species are typically not available via the silyl anion route, because of the limited availability of appropriate silyl anion reagents.<sup>5</sup> This synthetic method is therefore expected to greatly enhance further studies of early transition-metal silyl chemistry.

In the dark, benzene-*d*<sub>6</sub> solutions of zirconium silyl CpCp\*Zr[Si(SiMe<sub>3</sub>)<sub>3</sub>]Cl<sup>6</sup> (**1**, Cp =  $\eta^5$ -C<sub>5</sub>H<sub>5</sub>; Cp\* =  $\eta^5$ -C<sub>5</sub>Me<sub>5</sub>) react with PhSiH<sub>3</sub> over 6 h to give four products identified by <sup>1</sup>H NMR spectroscopy (eq 2). Early in the reaction, the major



products are zirconium silyl **2**<sup>7</sup> and HSi(SiMe<sub>3</sub>)<sub>3</sub>. As the reaction proceeds to completion, **2** decomposes to hydride **3** and a mixture of polysilanes. Broad <sup>1</sup>H and <sup>29</sup>Si NMR resonances for the polysilanes were assigned based on comparisons to spectra reported by Aitken et al.<sup>2a</sup> and to isolated (SiHPh)<sub>n</sub> polymer.<sup>2</sup> We have not isolated enough of this polymeric material to carry out molecular weight measurements, but it is evident from <sup>1</sup>H NMR spectra that PhH<sub>2</sub>SiSiH<sub>2</sub>Ph and PhH<sub>2</sub>SiSiHPhSiH<sub>2</sub>Ph are not present. In the presence of fluorescent room light, the reaction between **1** and PhSiH<sub>3</sub> is complete within 5 min and gives **2** and HSi(SiMe<sub>3</sub>)<sub>3</sub> cleanly. Compound **2** then slowly decomposes to **3** and (SiHPh)<sub>n</sub>.

Because analogous  $\sigma$ -bond metathesis reactions with CpCp\*Hf[Si(SiMe<sub>3</sub>)<sub>3</sub>]Cl<sup>6</sup> (**4**) give more stable metal silyl derivatives, these reactions were examined in more detail. As expected, the thermal (dark) reaction of **4** with 1 equiv of PhSiH<sub>3</sub> is much slower than observed for **1** (complete reaction after 2 days at room temperature). With illumination by fluorescent room lighting, this reaction is complete within 1 h in pentane or benzene solution, giving quantitative conversion to the  $\sigma$ -bond metathesis products CpCp\*Hf(SiH<sub>2</sub>Ph)Cl (**5**) and HSi(SiMe<sub>3</sub>)<sub>3</sub> (eq 3). In



contrast to **2**, yellow crystalline **5** is stable indefinitely as a solid at room temperature under an inert atmosphere. When heated to 75 °C in benzene-*d*<sub>6</sub>, **5** decomposes by a second-order process ( $k(75\text{ °C}) = 1.1(1) \times 10^{-4} \text{ M}^{-1} \text{ s}^{-1}$ ;  $\Delta H^\ddagger = 19.5(2) \text{ kcal mol}^{-1}$ ;  $\Delta S^\ddagger = -21.2(6) \text{ eu}$ ) to cleanly produce [CpCp\*HfHCl]<sub>2</sub> and (SiHPh)<sub>n</sub>. Compound **5** was completely characterized by analytical and spectroscopic data.<sup>7</sup> NMR chemical shifts for the diastereotopic hydrogens on silicon ( $\delta$  4.68, 5.14) and the <sup>1</sup>J<sub>SiH</sub> coupling constant (150 Hz) are consistent with bonding of the silyl group to a chiral, d<sup>0</sup> metal center.<sup>5</sup> Further study of the latter reaction should provide mechanistic information relevant to the catalytic dehydrogenative polymerization of silanes to polysilanes.

A number of new hafnium silyl derivatives have been obtained by reaction of **4** with 1 equiv of a primary or secondary silane (RSiH<sub>3</sub>, R = Ph, *p*-MeC<sub>6</sub>H<sub>4</sub>, 2,4,6-Me<sub>3</sub>C<sub>6</sub>H<sub>2</sub>, CH<sub>2</sub>Ph, and *c*-C<sub>6</sub>H<sub>11</sub>; Ph<sub>2</sub>SiH<sub>2</sub>; PhMeSiH<sub>2</sub>). These reactions are quantitative by <sup>1</sup>H NMR spectroscopy, and isolated yields range from 65–75%. For CpCp\*Hf(SiHPhMe)Cl, a 7:5 mixture of diastereomers are observed. Generally, the rates of these photochemical reactions are quite sensitive to steric effects. Secondary silanes and sterically hindered primary silanes such as (2,4,6-Me<sub>3</sub>C<sub>6</sub>H<sub>2</sub>)SiH<sub>3</sub> react sluggishly (over 1–2 days for 1:1 reactions) in the presence of room light. Tertiary silanes such as Me<sub>3</sub>SiH and Et<sub>3</sub>SiH react very slowly under analogous conditions, and as yet we have observed only small quantities of the HSi(SiMe<sub>3</sub>)<sub>3</sub> product after several days. Generally, hafnium silyls CpCp\*Hf(SiRR'R'')Cl undergo clean  $\sigma$ -bond metathesis reactions with primary or secondary silanes that introduce a smaller silyl ligand.

The thermal reactions of **1** and **4** with silanes may occur via four-center transition states, similar to those recently described

(1) Tilley, T. D. In *The Chemistry of Organic Silicon Compounds*; Patai, S., Rappoport, Z., Eds.; Wiley: New York, 1989; Chapter 24, p 1415.

(2) (a) Aitken, C.; Harrod, J. F.; Gill, U. S. *Can. J. Chem.* **1987**, *65*, 1804. (b) Aitken, C. T.; Harrod, J. F.; Samuel, E. *J. Am. Chem. Soc.* **1986**, *108*, 4059. (c) Aitken, C.; Harrod, J. F.; Samuel, E. *Can. J. Chem.* **1986**, *64*, 1677. (d) Harrod, J. F. In *Inorganic and Organometallic Polymers*; Zeldin, M., Wynne, K. J., Allcock, H. R., Eds.; ACS Symposium Series 360; American Chemical Society: Washington DC, 1988; Chapter 7.

(3) For a recent review of polysilane polymers, see: West, R. *J. Organomet. Chem.* **1986**, *300*, 327.

(4) (a) Trefonas, P., III; West, R.; Miller, R. D. *J. Am. Chem. Soc.* **1985**, *107*, 2737. (b) Harrah, L. A.; Zeigler, J. M. *Macromolecules* **1987**, *20*, 601. (c) Kepler, R. G.; Zeigler, J. M.; Harrah, L. A.; Kurtz, S. R. *Bull. Am. Phys. Soc.* **1983**, *28*, 362. (d) West, R.; David, L. D.; Djurovich, P. I.; Stearley, K. L.; Srinivasan, K. S. V.; Yu, H. *J. Am. Chem. Soc.* **1981**, *103*, 7352. (e) Yajima, S. *Am. Ceram. Soc. Bull.* **1983**, *62*, 893. (f) West, R.; David, L. D.; Djurovich, P. I.; Yu, H. *Am. Ceram. Soc. Bull.* **1983**, *62*, 899. (g) Schilling, C. L., Jr.; Wesson, J. P.; Williams, T. C. *Am. Ceram. Soc. Bull.* **1983**, *62*, 912. (h) Kajzar, F.; Messier, J.; Rosilio, C. *J. Appl. Phys.* **1986**, *60*, 3040.

(5) Roddick, D. M.; Heyn, R. H.; Tilley, T. D. *Organometallics* **1989**, *8*, 324.

(6) Elsner, F. H.; Tilley, T. D.; Rheingold, A. L.; Geib, S. J. *J. Organomet. Chem.* **1988**, *358*, 169. The hafnium derivative **4** was prepared analogously.

(7) Characterization data for all new compounds are listed in the Supplementary Material. Selected data for **2**: <sup>1</sup>H NMR (benzene-*d*<sub>6</sub>, 22 °C, 300 MHz)  $\delta$  1.73 (s, 15 H, C<sub>5</sub>Me<sub>5</sub>), 4.27 (d, <sup>2</sup>J<sub>HH</sub> = 1.2 Hz, 1 H, SiH), 4.70 (d, <sup>2</sup>J<sub>HH</sub> = 1.2 Hz, 1 H, SiH), 5.66 (s, 5 H, C<sub>5</sub>H<sub>5</sub>); <sup>29</sup>Si NMR (benzene-*d*<sub>6</sub>, 22 °C, 59.6 MHz)  $\delta$  -14.33 (t, <sup>1</sup>J<sub>SiH</sub> = 144 Hz). For **3**, prepared independently from **1** and H<sub>2</sub>: IR 1595 m (Zr-H); <sup>1</sup>H NMR (benzene-*d*<sub>6</sub>, 22 °C, 300 MHz)  $\delta$  1.84 (s, 15 H, C<sub>5</sub>Me<sub>5</sub>), 5.85 (s, 5 H, C<sub>5</sub>H<sub>5</sub>), 6.59 (s, 1 H, ZrH). For **5**: IR 2050 s (Si-H); <sup>1</sup>H NMR (benzene-*d*<sub>6</sub>, 22 °C, 300 MHz)  $\delta$  1.81 (s, 15 H, C<sub>5</sub>Me<sub>5</sub>), 4.68 (d, <sup>2</sup>J<sub>HH</sub> = 1.2 Hz, 1 H, SiH), 5.14 (d, <sup>2</sup>J<sub>HH</sub> = 1.2 Hz, 1 H, SiH), 5.63 (s, 5 H, C<sub>5</sub>H<sub>5</sub>); <sup>29</sup>Si NMR (benzene-*d*<sub>6</sub>, 22 °C, 59.6 MHz)  $\delta$  1.49 (t, <sup>1</sup>J<sub>SiH</sub> = 150 Hz).